

Quantum Manifestations of Chaotic Scattering

Ying-Cheng Lai,^{(1),(2)} Reinhold Blümel,⁽³⁾ Edward Ott,^{(1),(2),(4)} and Celso Grebogi^{(1),(5)}

⁽¹⁾Laboratory for Plasma Research, University of Maryland, College Park, Maryland 20742

⁽²⁾Department of Physics and Astronomy, University of Maryland, College Park, Maryland 20742

⁽³⁾Department of Physics and Astronomy, University of Delaware, Newark, Delaware 19716

⁽⁴⁾Department of Electrical Engineering, University of Maryland, College Park, Maryland 20742

⁽⁵⁾Institute for Physical Science and Technology and Department of Mathematics, University of Maryland, College Park, Maryland 20742

(Received 24 March 1992)

We examine quantum chaotic scattering in the semiclassical regime for the two cases where the classical scattering is hyperbolic and nonhyperbolic. It is shown that in the nonhyperbolic case the energy-dependent S -matrix autocorrelation function $C(\varepsilon)$ exhibits a cusp-shaped peak at $\varepsilon=0$ (where ε denotes the energy difference). This indicates that the fine scale fluctuations with energy of the S matrix are characteristically greatly enhanced in the nonhyperbolic case as compared with the hyperbolic case.

PACS numbers: 05.45.+b, 03.80.+r, 11.20.-e, 42.50.Lc

Chaotic scattering has been found in a large variety of classical physical systems [1-3]. The dynamics in such cases may be characterized as either *hyperbolic* or *nonhyperbolic*. In hyperbolic chaotic scattering, all the periodic orbits are unstable and there are no Kolmogorov-Arnold-Moser (KAM) surfaces in the scattering region. In this case, the survival probability of a particle in the scattering region typically decays exponentially [1,2] with time $P(E,t) \sim \exp(-\gamma t)$, where t denotes time and E denotes energy. On the other hand, in nonhyperbolic chaotic scattering, there are both KAM surfaces and chaotic regions in the phase space [3]. A particle initialized in the chaotic region can spend a long time in the vicinity of KAM surfaces. In this case, current evidence indicates that the survival probability of a particle decays roughly algebraically [4] with time $P(E,t) \sim t^{-z}$ for large t . Recently, studies on quantum manifestations of hyperbolic chaotic scattering [5] show that the elements $S_{ij}(E)$ of the quantum scattering matrix (S matrix) exhibit fluctuations in their dependence on the energy [5]. In this Letter we consider both hyperbolic and nonhyperbolic chaotic scattering and show that the fine scale semiclassical quantum fluctuations of the S matrix with energy are characteristically greatly enhanced in the nonhyperbolic case as compared with the hyperbolic case.

The energy autocorrelation function of an S -matrix element is defined as $C_{ij}(\varepsilon) = \langle S_{ij}^*(E) S_{ij}(E + \varepsilon) \rangle_E$, where ε is the energy difference (small) and $\langle \cdot \rangle_E$ denotes an average over a band of energies centered at some value $E = E_0$ and of width ΔE , where ΔE is classically small ($\Delta E/E_0 \ll 1$) but "quantum mechanically large" ($\Delta E \gg \varepsilon$). More specifically, we define the average by $\langle \cdots \rangle_E = (1/\Delta E) \int \cdots f((E - E_0)/\Delta E) dE$, where in our numerical work we take $f(x) = (1 - |x/\sqrt{6}|)/\sqrt{6}$ for $|x| < \sqrt{6}$ and $f(x) = 0$ for $|x| \geq \sqrt{6}$.

To evaluate $C_{ij}(\varepsilon)$, we use the semiclassical approxi-

mation in which the S -matrix elements are given by [6]

$$S_{ij}(E) = \sum_s [P_{j \rightarrow i}^{(s)}(E)]^{1/2} \exp \left[\frac{i}{\hbar} \Phi^{(s)}(E) - \frac{i\pi}{2} \nu^{(s)} \right], \quad (1)$$

where (s) denotes a classical path, $P_{j \rightarrow i}^{(s)}(E)$ is the classical transition probability from state j to state i along the path s , $\Phi^{(s)}(E)$ is the classical (reduced) action along the path (s) , and $\nu^{(s)}$ is the Maslov index. The sum is over all the classical paths connecting state j and state i . The classical transition probability is given by [6] $P_{j \rightarrow i}^{(s)}(E) = (1/2\pi) |\partial I_i / \partial \theta_j|_s^{-1}$, where (I_j, θ_j) and (I_i, θ_i) are the action-angle variables in the states j and i , respectively. For chaotic scattering, the number of classical paths connecting j and i increases exponentially with the length of the path. Hence, the sum in Eq. (1) is difficult to evaluate. Nonetheless, Eq. (1) is useful for the heuristic estimation of average quantities [5].

Substituting Eq. (1) into the definition of $C_{ij}(\varepsilon)$, approximating $\Phi^{(s)}(E + \varepsilon)$ as $\Phi^{(s)}(E) + \varepsilon \partial \Phi^{(s)} / \partial E$, and neglecting the contribution from cross terms in the double sum over the classical paths, we get [5]

$$C_{ij}(\varepsilon) \sim \int dt \langle P_{ij}(E, t) \rangle_E \exp(i\varepsilon t / \hbar), \quad (2)$$

where t is the delay time of the particle in the scattering region. In Eq. (2), $P_{ij}(E, t) dt$ is the classical probability that a $j \rightarrow i$ transition occurs while the delay time is in the interval $[t, t + dt]$. For hyperbolic chaotic scattering, $P_{ij}(E, t) \sim P(E, t) \sim \exp(-\gamma t)$. Substituting this exponential law into Eq. (2), we obtain [5]

$$C(\varepsilon) \sim 1/(\varepsilon/\hbar + i\gamma), \quad (3)$$

which is Lorentzian. For small ε we have $|C(\varepsilon)|_{\varepsilon \rightarrow 0} \approx \text{const} + O(\varepsilon^2)$. For nonhyperbolic chaotic scattering,

$P(E,t) \sim t^{-z}$ for large t . Substituting this algebraic law into Eq. (2), we can evaluate the integral asymptotically for small ε . We obtain

$$C(\varepsilon) = C_0 + C_1(\varepsilon/\hbar)^{z-1}, \tag{4}$$

where $C(\varepsilon) \equiv |C_{ij}(\varepsilon)|$, $C_0 \equiv C(0)$, and C_1 is a negative constant.

From Eq. (4), we observe that $dC(\varepsilon)/d\varepsilon \sim (\varepsilon/\hbar)^{z-2}$. So in typical cases where $1 < z < 2$ ($z \approx 1.45$ in Karney's numerical experiment [4], $z \approx 1.34$ in Chirikov and Shepelyansky's numerical experiment [4], $z < 1.96$ in a theory based on a Markov-Tree model by Meiss and Ott [4]), we have $dC(\varepsilon)/d\varepsilon|_{\varepsilon \rightarrow 0} \rightarrow \infty$. Hence, the energy autocorrelation function exhibits a cusp near $\varepsilon=0$. That is, $C(\varepsilon)$ decreases very rapidly from $\varepsilon=0$.

The above argument for the existence of Lorentzian behavior of $C(\varepsilon)$ in hyperbolic chaotic scattering and the cusp behavior of $C(\varepsilon)$ in nonhyperbolic chaotic scattering is nonrigorous since it involves the long time limit of the semiclassical approximation [7]. Thus we have undertaken a series of numerical experiments to test Eqs. (3) and (4). We consider a system in which particles are scattered from a two-dimensional array of nonoverlapping, elastic scatterers in the plane [2]. These scatterers are placed at constant intervals D along the y axis and each scatterer is represented by a circular attractive potential $V(r)$ that becomes negligibly small for $r > R$, where $R < D/2$. Classically, the effect of an individual scatterer on a scattering particle can be characterized by the elastic deflection angle $\Theta(l)$ as a function of the angular momentum l . Note that $\Theta(l)$ vanishes for $l > l_{\max} = uR$ (mass of the particle = 1) due to the finite range of the potential, where u is the particle velocity in the region where the potential is negligible. For $V(r)$ we choose the Woods-Saxon potential [8] $V(r) = -V_0/(1 + \exp[(r - R_0)/a])$, where $V_0 > 0$ and R_0 and a are constants. We choose the angular momentum l and angle β as the dynamical variables [2], where β is the angle of a particle trajectory relative to the $-y$ axis when the particle is in regions where the potential is negligible. We define a mapping that relates (l, β) with respect to a scatterer to (l', β') with respect to the next scatterer after the particle's being scattered from the first scatterer. The mapping can be explicitly expressed as [2] $\beta' = \beta + \Theta(l) \pmod{2\pi}$ and $l' = l - (Du) \text{sgn}(\cos\beta') \sin\beta'$, if $|l'| \leq l_{\max}$ and, if $|l'| > l_{\max}$, the particle exits the system.

We fix $V_0=10$, $R_0=1$, $a=0.1$, and $D=4$. Thus, $V(r=D/2)/V_0 \sim 10^{-5}$ so in practice the adjacent potentials do not overlap each other. When the particle energy is large, we observe that the phase space consists of KAM islands and chaotic regions, as shown in Fig. 1(a) for $E=10$ (the chaotic invariant set is numerically obtained by the "sprinkler" method [9]). In this case, the scattering is nonhyperbolic and the decay of particles from the scattering region is well fitted by an algebraic dependence over the time range tested with a decay exponent of

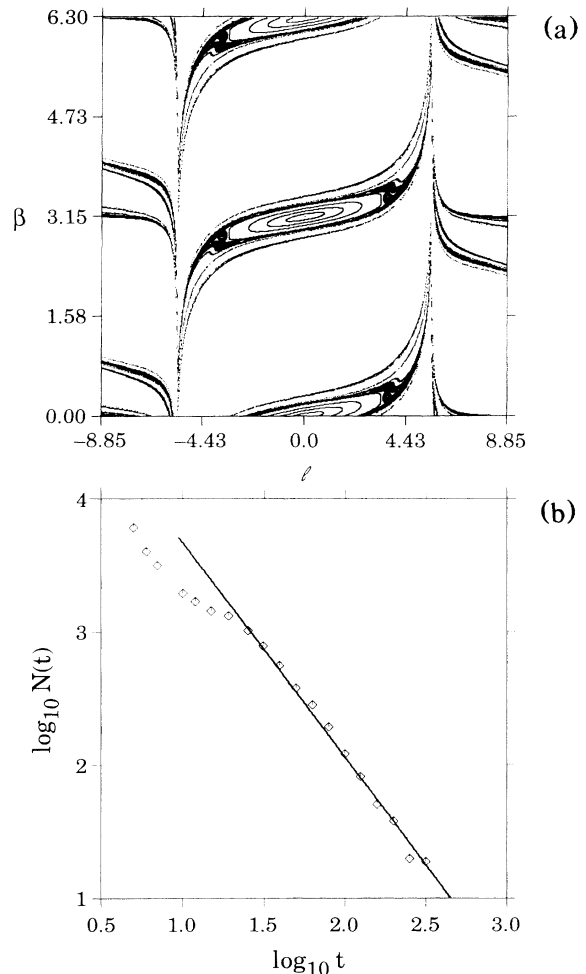


FIG. 1. Nonhyperbolic chaotic scattering for $E=10$: (a) chaotic invariant sets and KAM islands and (b) $\log_{10}N(t)$ vs $\log_{10}t$.

$z \approx 1.62$, as shown in Fig. 1(b). To calculate the decay curve in Fig. 1(b), we initialize a large number of particles uniformly distributed in the region ($l \in [4.5, 6.5]$, $\beta \in [0, 2\pi]$) which apparently does not contain KAM islands and record the number of particles $N(t)$ that have not escaped the scattering region at time t . As the particle energy decreases from $E=10$ to $E=E_{\text{crit}}$ ($1 < E_{\text{crit}} < 10$), the KAM surfaces are destroyed. At lower values of E , we find numerically that there are no KAM surfaces and the decay of particles from the scattering region is exponential. In this case, the scattering is hyperbolic, as shown in Fig. 2(a) (the chaotic invariant set) and the semilogarithmic plot in Fig. 2(b) (exponential decay) for the case of $E=1$.

Quantum mechanically, the effect of any single scatterer is completely specified once the phase shifts $\sigma_l(E)$ are given [5]. Because of the discrete translational symmetry of the system in the y direction, the wave function satisfies $\psi^{(a)}(x, y) = \exp(ia y) \varphi^{(a)}(x, y)$, where $\varphi^{(a)}(x, y)$

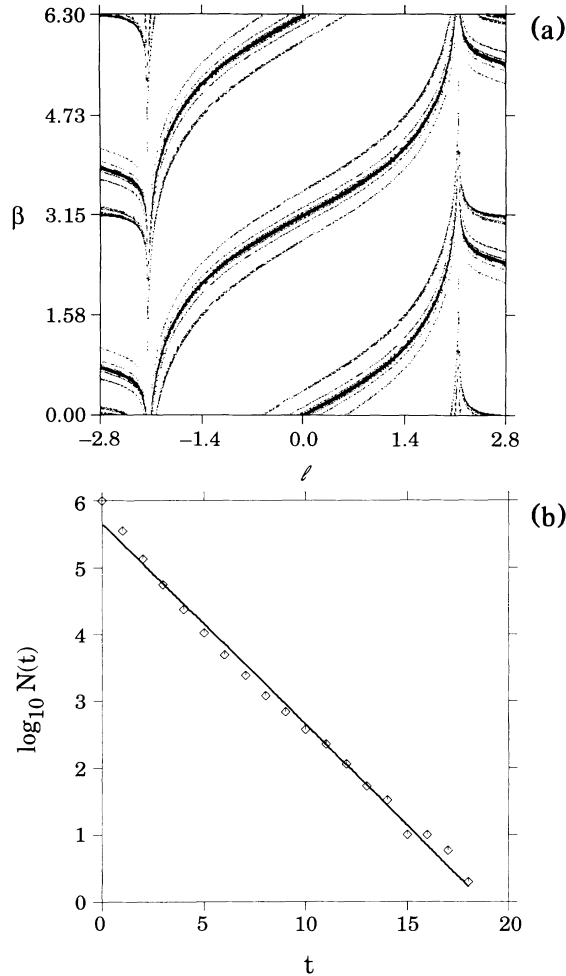


FIG. 2. Hyperbolic chaotic scattering for $E=1$: (a) the chaotic invariant set and (b) the exponential decay.

is D periodic in y . So we have $\psi^{(a)}(x, y+nD) = \exp(inaD)\psi^{(a)}(x, y)$. Thus the y component of the momentum q_n is quantized $q_n = \alpha + 2n\pi/D$. Since by the conservation of energy $q_n^2 \leq k^2$, where k is the wave vector for the energy [$E = (\hbar^2/2m)k^2$], there exists a maximum integer N_B (maximum number of open channels) above which q_n is not allowed and corresponds to evanescent waves. To calculate the quantum S matrix, we make use of the Koringa-Kohn-Rostoker method [10] adapted to the present problem [5].

To compare the quantum calculation with the semiclassical prediction of Eqs. (3) and (4), we must use sufficiently small values of Planck's constant \hbar , so that there are a large number of waves on the scale of the system length D . In the following, we shall compute results for a nonhyperbolic case, with nominal energy $E_0=10$, and a hyperbolic case with nominal energy $E_0=1$. For $E_0=10$, we choose $\hbar^2/2m = 10^{-3}$ so that the corresponding wave vector is $k_0=100$ and there are 127 open channels ($128 > 2D/\lambda > 127$). In the case of hyperbolic scattering where $E_0=1$, we choose $\hbar^2/2m = 10^{-4}$ (hence, we also

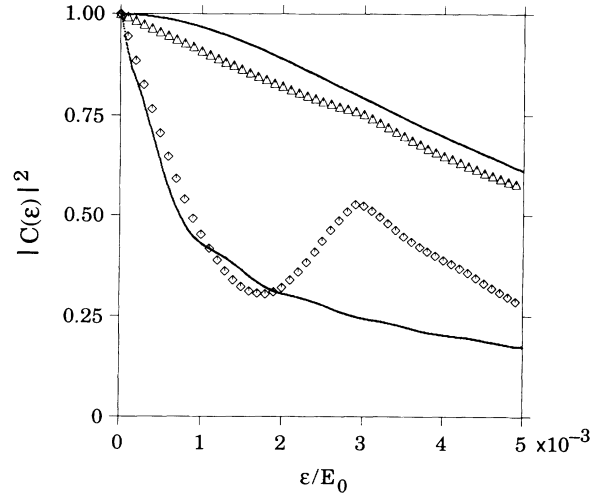


FIG. 3. Magnitude squared of S -matrix autocorrelation functions [diamonds for the nonhyperbolic case ($E_0=10$) and triangles for the hyperbolic case ($E_0=1$)] and the corresponding semiclassical predictions (the thick solid curves).

have $k_0=100$) so the number of open channels (127) is the same as that in our nonhyperbolic scattering case. We then calculate the autocorrelation function $C(\epsilon)$ using $\Delta E/E_0 \approx 0.1$. As a function of energy, an S -matrix element contains both a smooth part and a fluctuating part. To compare with the semiclassical theory, we subtract the smooth part and only keep the fluctuating part. Figure 3 shows the magnitude squared of the quantum autocorrelation functions $|C(\epsilon)|^2$ for both the $E_0=10$ case (nonhyperbolic, plotted as diamonds) and the $E_0=1$ case (hyperbolic, plotted as triangles). For Fig. 3, we also perform an average with respect to a small block of matrix elements around a combination i and j ($i=14$, $j=25$). We observe that the $C(\epsilon)$ curves thus obtained are essentially independent of i and j . Also shown in Fig. 3 are the semiclassical predictions from Eq. (2); the lower thick solid curve corresponds to $E_0=10$, and the upper thick solid curve corresponds to $E_0=1$. To calculate the semiclassical correlation functions, we use the classical decay data of Figs. 1(b) and 2(b) and substitute them directly into Eq. (2). From Fig. 3, we see that for the hyperbolic case, at small ϵ the energy autocorrelation function deviates somewhat from the semiclassical Lorentzian prediction. This deviation may result from the failure of the assumptions used in deriving Eq. (2) from the semiclassical expression Eq. (1) for our finite \hbar numerical calculation or from the failure of the validity of the long time limit of the semiclassical theory itself. For the nonhyperbolic case, Fig. 3 suggests that the quantum calculation agrees reasonably well with the semiclassical theory at small ϵ , and the energy autocorrelation function appears to follow the predicted cusp [11] near $\epsilon=0$. Even though the hyperbolic $C(\epsilon)$ function deviates from the predicted Lorentzian, its magnitude is still higher than that of the nonhyperbolic case. This means

that as compared with the hyperbolic scattering case, the fine scale fluctuations of S -matrix elements with energy are greatly enhanced in the nonhyperbolic case [12].

In conclusion, we have presented evidence that, in the semiclassical regime, the quantum energy autocorrelation function decreases more rapidly away from $\varepsilon=0$ in the case of nonhyperbolic chaotic scattering. *Thus the fine energy scale fluctuations of S -matrix elements are characteristically greatly enhanced in nonhyperbolic chaotic scattering as compared with the case of hyperbolic chaotic scattering.*

This work was supported by the Department of Energy (Scientific Computing Staff, Office of Energy Research) and by the Office of Naval Research (Physics). R.B. is grateful for the financial support by the Deutsch Forschungsgemeinschaft.

- [1] M. C. Gutzwiller, *Physica (Amsterdam)* **7D**, 341 (1983); D. W. Noid, S. Gray, and S. A. Rice, *J. Chem. Phys.* **84**, 2649 (1986); C. Jung, *J. Phys. A* **19**, 1345 (1986); M. Hénon, *Icarus* **66**, 536 (1986); *Physica (Amsterdam)* **33D**, 132 (1988); B. Eckhardt and H. Aref, *Trans. Soc. R. London A* **326**, 655 (1988); B. Eckhardt, *Europhys. Lett.* **61**, 329 (1988); P. Gaspard and S. A. Rice, *J. Chem. Phys.* **90**, 2225 (1989); S. Bleher, E. Ott, and C. Grebogi, *Phys. Rev. Lett.* **63**, 919 (1989); Z. Kovács and T. Tél, *Phys. Rev. Lett.* **64**, 1617 (1990).
- [2] G. Troll and U. Smilansky, *Physica (Amsterdam)* **35D**, 34 (1989).
- [3] M. Ding, C. Grebogi, E. Ott, and J. A. Yorke, *Phys. Rev. A* **42**, 7025 (1990); Y. T. Lau, J. M. Finn, and E. Ott, *Phys. Rev. Lett.* **66**, 978 (1991).
- [4] J. D. Meiss, J. R. Cary, C. Grebogi, J. D. Crawford, A. N. Kaufman, and H. D. I. Abarbanel, *Physica (Amsterdam)* **6D**, 375 (1983); C. F. F. Karney, *Physica (Amsterdam)* **8D**, 360 (1983); B. V. Chirikov and D. L. Shepelyansky, *Physica (Amsterdam)* **13D**, 395 (1984); J. D. Meiss and E. Ott, *Phys. Rev. Lett.* **55**, 2741 (1985); M. Ding, T. Bountis, and E. Ott, *Phys. Lett. A* **151**, 395 (1990).
- [5] R. Blümel and U. Smilansky, *Phys. Rev. Lett.* **60**, 477 (1988); *Physica (Amsterdam)* **36D**, 111 (1989); R. Blümel, B. Dietz, C. Jung, and U. Smilansky, *J. Phys. A* (to be published).
- [6] W. H. Miller, *Adv. Chem. Phys.* **30**, 77 (1975).
- [7] The cusp behavior, Eq. (4), holds only in the range $\varepsilon_{\max} \geq \varepsilon \geq \varepsilon_{\min}$, where $\varepsilon_{\max} \sim \hbar/t_1$ and t_1 is the classically determined time past which the power-law form for $P(E, t)$ holds [cf. Fig. 1(b)]. The cutoff of the cusp behavior at very small energy difference ε_{\min} occurs because the semiclassical approximation breaks down at long times $t \gtrsim t_2$ corresponding to $\varepsilon_{\min} \sim \hbar/t_2$. In particular, the power-law decay results from particle orbits that spend long stretches of time near KAM surfaces. Orbits contributing to longer times penetrate more deeply into the sticky region near a KAM surface. At finite wavelength, there comes a time past which the phase-space structures resolved by classical orbits still in the scattering region are quantum mechanically not resolved. This determines the time t_2 . Y. C. Lai, E. Ott, and C. Grebogi (to be published), and also Y. C. Lai [Ph.D. thesis (unpublished)] estimate t_2 using the Markov chain model of J. D. Hanson, J. R. Cray, and J. D. Meiss [*J. Stat. Phys.* **39**, 327 (1985)] and find that the scaling $t_2 \sim \hbar^{-\mu}$, with μ a positive number. This same scaling has been previously found for the quantum kicked rotor at the critical classical parameter value for the onset of global chaos by S. Fishman, D. R. Grempel, and R. E. Prange [*Phys. Rev. A* **36**, 289 (1987)] by means of a renormalization-group analysis. As ε decreases through ε_{\min} the magnitude of the correlation function must turn over and reach $\varepsilon=0$ with zero slope. This is a consequence of the fact that scattering coefficients are smooth on a sufficiently small energy scale. Thus for very small ε , $S_{ij}(E+\varepsilon)$ can be expanded as $S_{ij}(E+\varepsilon) \cong S_{ij}(E) + \varepsilon dS_{ij}/dE + (\varepsilon^2/2)d^2S_{ij}/dE^2$. Substituting the expansion for $S_{ij}(E+\varepsilon)$ into Eq. (1) and noting that, for continuous weighting function $f(x)$, $\text{Re}\langle S_{ij}^* dS_{ij}/dE \rangle_E = \langle |S_{ij}|^2/dE \rangle_E$ goes to zero in the semiclassical limit ($\hbar \rightarrow 0$), we obtain for $|C(\varepsilon)|$ the small ε dependence, $C_0 + C_1\varepsilon^2$. The region $\varepsilon < \varepsilon_{\min}$ is apparently not resolved in our numerical experiments.
- [8] R. D. Woods and D. S. Saxon, *Phys. Rev.* **95**, 577 (1954).
- [9] H. Kantz and P. Grassberger, *Physica (Amsterdam)* **17D**, 75 (1985); G. Hsu, E. Ott, and C. Grebogi, *Phys. Lett.* **127**, 199 (1988).
- [10] J. Koringa, *Physica (Utrecht)* **13**, 392 (1947); W. Kohn and N. Rostoker, *Phys. Rev.* **94**, 1111 (1954); M. V. Berry, *Ann. Phys. (N.Y.)* **131**, 163 (1981).
- [11] R. A. Jalabert, H. U. Baranger, and A. Douglas Stone [Phys. Rev. Lett. **65**, 2442 (1990), and following publications and seminars] considered the difference between a chaotic stadium billiard and a nonchaotic polygonal billiard (no KAM surfaces) using a semiclassical argument. Also, for a case where the classical scattering yields a power-law decay, C. H. Lewenkopf [Ph.D. thesis, University of Heidelberg, 1991 (unpublished)] has independently noted that the energy correlation function of his numerically computed S -matrix elements appears to be different from the Lorentzian form.
- [12] We also see that, in the nonhyperbolic case, there is a broad peaked feature centered at around $\varepsilon/E_0 \approx 3 \times 10^{-3}$. This may be due to the quantum scattering wave-function tunneling to the KAM island seen in Fig. 1(a) which can itself sustain slowly decaying metastable quantum states.